J. Steroid Biochem. Molec. Biol. Vol. 39, No. 4A, pp. 419–432, 1991
Printed in Great Britain.

0960-0760/91 $3.00 + 0.00

EVIDENCE FOR COLOCALIZATION OF GLUCOCORTICOID RECEPTOR WITH CYTOPLASMIC MICROTUBULES IN HUMAN GINGIVAL FIBROBLASTS, USING TWO DIFFERENT MONOCLONAL ANTI-GR ANTIBODIES, CONFOCAL LASER SCANNING MICROSCOPY AND IMAGE ANALYSIS

GUNNAR AKNER,[1]* KARIN MOSSBERG,[2] ANN-CHARLOTTE WIKSTRÖM,[1] KARL-GÖSTA SUNDQVIST[3] and JAN-ÅKE GUSTAFSSON[1]

[1]Department of Medical Nutrition, Karolinska Institute, Novum F-60, Huddinge University Hospital, 141 86 Huddinge, [2]Physics IV, The Royal Institute of Technology, 100 44 Stockholm and [3]Department of Clinical Immunology, Karolinska Institute, Huddinge University Hospital, Novum F-60, 141 86 Huddinge, Sweden

(Received 9 March 1991)

Summary—The cellular distribution of the glucocorticoid receptor (GR) in relation to the microtubule protein tubulin was studied in human gingival fibroblasts, using two different anti-GR antibodies of different Ig-classes, by indirect immunofluorescence immunocytology. Further studies were performed by confocal laser scanning microscopy and digital image analysis. The study focused on fluorochrome separation, optical sectioning, digital subtraction techniques and reconstruction of projections obtained using stacks of recorded transversal sections. The data presented further strengthens the notion of a structural colocalization between GR and cytoplasmic microtubules in human fibroblasts.

INTRODUCTION

The unliganded glucocorticoid receptor (GR) is recovered in the supernatant after high speed centrifugation of cellular homogenates, i.e. the cytosol [1], and GR has therefore been described as a cytosolic protein. Whether the cytosolic presence of unliganded GR corresponds to a cytoplasmatic localization of this receptor has been much debated in the light of the overall nuclear localization of among others the estrogen and progestin receptors [2]. However, by immunocytochemical studies conducted by ourselves [3–5] and others [6] we now consider the extranuclear localization of GR to be established. In addition, a part of the GR-pool resides in the nucleus.

The fact that unliganded GR is recovered in the cytosol does not necessarily mean that GR is a freely diffusing, water soluble macromolecule. There are indications that the intracellular distribution of GR is regulated or controlled in some way. The compartment shift of GR from the cytoplasm to the cell nucleus following binding of a glucocorticoid ligand is quite fast with a $t_{1/2}$ of about 5 min in monkey COS7 or CV-1 cells [6]. This may imply that a specific transport mechanism is in operation for efficient intranuclear transport of GR.

We have recently presented results indicating a structural codistribution between GR and cytoplasmic microtubules (MTs) in normal human, gingival fibroblasts [3]. Although evidence for a functional significance of this interaction is still lacking, the biological implications of a codistribution between GR and MTs are so far-reaching, that it is essential to confirm this finding using several experimental approaches.

In this paper, we extend our studies on the colocalization between GR and cytoplasmic MTs using two different monoclonal anti-GR antibodies and confocal laser scanning microscopy (CLSM). This technique allows optical sectioning of the specimen and reconstruction of the cell from a stack of optical sections. Thus, it is possible to artificially rotate a cell to any chosen angle, for instance to a side view projection. Furthermore, subtraction analysis allows a precise analysis of the colocalization of cellular

*To whom correspondence should be addressed.

structures stained with different specific antibodies and fluorochromes in the same section of a specimen. By performing this analysis it was possible to show that the staining pattern of GR and cytoplasmic MTs to a very large extent coincide.

EXPERIMENTAL

Cells and media

Cultures of normal human fibroblasts (originally biopsy-explants from the gingival mucosa) were subcultured as monolayers (passage 5–20) on glass cover-slips as previously described [3]. Cell media and supplementary components were purchased from Gibco (Uxbridge, Middlesex, England).

Manipulation of cell cultures

In some experiments, cells were cultured in the presence of 10 μM vinblastine for 1 h prior to fixation.

Antibodies

The following primary antibodies were used: A monoclonal mouse-anti-rat liver GR IgG2a antibody designated "mab 7" [7] in ascites, diluted 1/100, yielding a final protein concentration of 0.26 mg/ml. This antibody cross-reacts with the human GR [8]; a monoclonal mouse-anti-rat liver GR (IgM) antibody designated "mab 1" [7] in ascites, diluted 1/100, yielding a final protein concentration of 0.20 mg/ml. "Mab 1" recognizes a different epitope on GR than "mab 7" [7]; a polyclonal rabbit-anti-sea urchin egg tubulin heterodimer antibody (Dakopatts, Glostrup, Denmark) in serum, diluted 1/100, yielding a final protein concentration of 0.51 mg/ml; and a monoclonal mouse-anti-chick brain-beta-tubulin monomer antibody (Amersham Int. plc, England), diluted 1/100, yielding a final protein concentration of 0.075 mg/ml.

The following secondary antibodies were used: An FITC-conjugated goat-anti-mouse-Ig antibody (Becton Dickinson, Mountain View, CA, U.S.A.), diluted 1/10, yielding a final protein concentration of 0.025 mg/ml; and a Texas Red®-conjugated donkey-anti-rabbit-Ig antibody (Amersham Int.) diluted 1/25, yielding a final protein concentration of 0.020 mg/ml.

Immunostaining procedure

Indirect immunofluorescence and the double staining technique was used as described previously [3]. Briefly, cells were grown on sterile glass cover slips and after fixation in cold methanol (−20°C) for 10 min, cells were incubated with a mixture of the two primary antibodies for 60 min at room temperature. After washes in phosphate buffered saline (PBS), a mixture of the two secondary fluorochrome-conjugated antibodies was added and incubation was performed for 60 min. After washes in PBS, the cover slips were mounted upside down on glass slides (MenzelGläser, Braunschweig, Fed. Rep. Germany) in 50% glycerol in PBS.

As fluorochromes we used fluorescein-isothiocyanate (FITC) and Texas Red®; anti-GR being labeled by the green-emitting fluorochrome FITC and anti-tubulin by the red-emitting fluorochrome Texas Red®. These fluorochromes show a low amount of overlap [9] and can therefore be detected essentially independently of one another in the same cell.

Chemicals

Vinblastine was an analytical grade product from Sigma (St Louis, MO, U.S.A.).

CLSM

CLSM is based on the principle that out-of-focus contributions can be reduced by a point illuminating/point detection technique [10]. The technique results in an improved resolution compared with conventional microscopy and also in a pronounced depth discrimination, allowing recording of thin optical layers of a specimen. By recording subsequent images with a slight shift in focus, a data volume is produced, which can be used for three-dimensional (3D) reconstructions. The CLSM in this study was carried out with the PHOIBOS instrument, developed at Physics IV (The Royal Institute of Technology, Stockholm, Sweden) [11, 12]. An argon laser was used as the light source (Coherent Innova 70) providing eight selectable wavelengths in the interval of 458–514 nm.

The depth discrimination of the CLSM is due to the pronounced fall-off in light intensity when a specimen layer is defocused. The FWHM (full-width half-maximum) of the fall-off along the optical axis can be used as a measure of the "thickness' of an optical layer. The FWHM-value depends on the numerical aperture (NA) of the objective, the refractive index of the immersion medium and the wavelength of the light. In practice, we have measured the FWHM-value to 2.0 μm for an oil immersion $\times$40/1.0 NA objective and to 1.0 μm for an oil

immersion ×63/1.4 NA objective at a fluorescent wavelength of 550 nm. All images, except where otherwise indicated, were scanned using the ×63 objective.

Separation of the fluorochromes

To separate the fluorescent light from FITC and Texas Red® in double stained specimens, the samples were scanned twice with different excitation wavelengths and filter combinations. In this study, one volume (stack of optical sections) was recorded for each fluorochrome, with change of excitation wavelength and filters after completion of one full stack.

Figure 1 shows the excitation [Fig. 1(a)] and emission [Fig. 1(b)] spectra for FITC and Texas Red® measured according to Titus *et al.* [9]. Since we have used a different laser to Titus *et al.*, we have neither used the same excitation wavelengths, nor the same emission detection intervals, and thus we cannot expect a precise agreement with their data. There may also be slight changes in the spectral properties of the fluorochromes depending on which substances they are bound to and on their chemical surroundings. The spectra in Fig. 1 must therefore be interpreted with care. It should also be noted that the spectra are normalized and that the relative strength between the two fluorochromes may vary. A discussion on how the spectra are influenced by different variables is found in [13].

The spectra of FITC and Texas Red® are essentially non-overlapping, which indicates that a proper choice of excitation wavelengths gives a good separation of the emitted light from the fluorochromes. In the CLSM, a wavelength of 514 nm, the longest wavelength available from the argon laser, was used when detecting Texas Red®. The emission was surprisingly good considering the small amount of the fluorochrome that was excited [Fig. 1(a)]. A high-pass filter at 610 nm was used in front of the detector to cut off the emission light from FITC, still allowing parts of the Texas Red® emission to be detected [marked in Fig. 1(b)]. When detecting FITC, an excitation wavelength of 476 nm was used [indicated in Fig. 1(a)]. The wavelength was chosen to give as strong an FITC-signal as possible, while at the same time the Texas Red®-signal was kept low. A 500 nm low-pass filter combined with a 550 nm high-pass filter was used to detect the wavelength interval 500–550 nm, as indicated in Fig. 1(b). No mathematical corrections were used to improve the separations of the two fluorochromes in the images.

Image analysis

The digital data volume recorded by the microscope was inspected by projecting the entire or parts of the volume on a two-dimensional image. The projections were calculated from different angles to show the volume from different views [14]. To compare the relative distributions of FITC and Texas Red®, two images (F and T) were recorded from the same optical section. The background levels in the images were measured by encircling areas only containing background. The mean values of these areas were calculated and removed

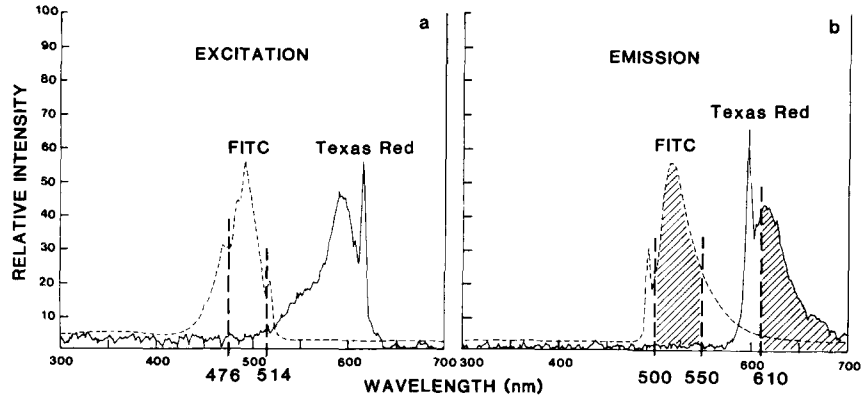

Fig. 1. Normalized absorption (a) and emission (b) spectra for FITC (---) and Texas Red® (——), measured by Titus *et al.*, 1982 [9]. The fluorochromes are conjugated to goat-anti-rabbit IgG antibodies. (a) The wavelength of the monochromatic excitation light was varied and the intensity of the emitted light was recorded at the wavelength 517 nm (FITC) and 615 nm (Texas Red®). The laser excitation wavelengths used in our study to excite FITC (476 nm) and Texas Red® (514 nm) are indicated by dotted lines. (b) The emitted light recorded using a constant excitation wavelength of 492 nm (FITC) and 596 nm (Texas Red®). The emission detection intervals in our study are indicated: FITC 500–550 nm, Texas Red® >610 nm.

from the original images. The remaining image intensities were then considered to represent only the specific staining signal. To make a comparison between the distribution of FITC and Texas Red®, the total intensities in the images were equalized by multiplying all picture elements in one of the images by a constant factor. Two new images were then created that showed one fluorochrome subtracted from the other and vice versa (F – T) and (T – F). Negative pixel values were set to zero.

Photography

Microphotography was performed as described in [3] for the conventional immunostainings [Figs 3 and 7]. The inverted image on the TV-screen (Sun work station 386i) work was photographed by a Pentax ASAHI (KX)-camera using a Kodak TMAX black-and-white 100 ASA film at an ASA setting of 100 and exposure time setting of 0.5 s.

RESULTS

Specificity

In a previous paper [3], we have shown by a whole cell ligand binding assay that the human gingival fibroblasts used in this study contain about 110,000 specific GR-molecules/cell and that this number is only slightly reduced to about 90,000 molecules/cell after 1 h treatment with vinblastine. All the primary antibodies recognized their own specific antigen (GR and tubulin, respectively) and showed no sign of cross-reactivity between GR and tubulin in Western immunoblotting experiments [3]. Control antibodies against various intracellular and plasma membrane structures showed the expected immunocytochemical patterns.

Separation of the fluorochromes

Figure 2 shows 1 μm thick optical transversal sections through the central part of two different fibroblasts, monostained for GR using FITC [Fig. 2(a)] and tubulin using Texas Red® [Fig. 2(d)]. In Fig. 2(b) and (c) the same cells are shown after scanning with the opposite filter combination. The fluorescence is not totally suppressed in Fig. 2(b) and (c), respectively, and this may be caused by a small amount of the fluorochromes being detected by the opposite filter combination (bleeding, cross-talk), but may also be due to autofluorescence. To determine the amount of cross-talk including autofluorescence that is seen in Fig. 2(b) and (c), the ratio of the total intensities of the images

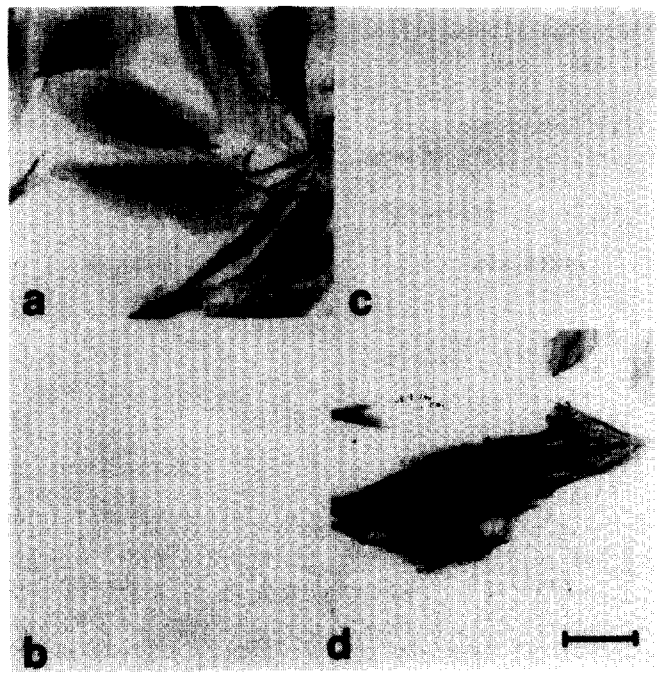

Fig. 2. CLSM separation of fluorochromes. (a and b) Interphase fibroblast monostained for GR scanned with FITC- (a) and Texas Red®-filter setting (b). (c) and (d) Interphase fibroblast monostained for tubulin scanned with Texas Red®- (d) and FITC-filter setting (c). The cross-talk including autofluorescence is very low, calculated to be 3% for FITC and 5% for Texas Red®. The image was scanned using the ×40 objective. Bar corresponds to 60 μm.

was calculated after the background had been removed. The cross-talk from FITC in Fig. 2(b) was calculated to be 3% and from Texas Red® in Fig. 2(c), 5%.

Interphase cells during basal culture conditions

The cellular distribution of GR and tubulin in conventional immunofluorescence double staining microscopy using the two different monoclonal anti-GR antibodies "mab 7" and "mab 1", and a polyclonal anti-tubulin antibody is shown in Fig. 3. The IgM GR-antibody "mab 1" showed a very similar staining pattern as described previously for the IgG "mab 7" [3]. GR was predominantly found in the cytoplasm, where it exhibited a fibrillar pattern correlating

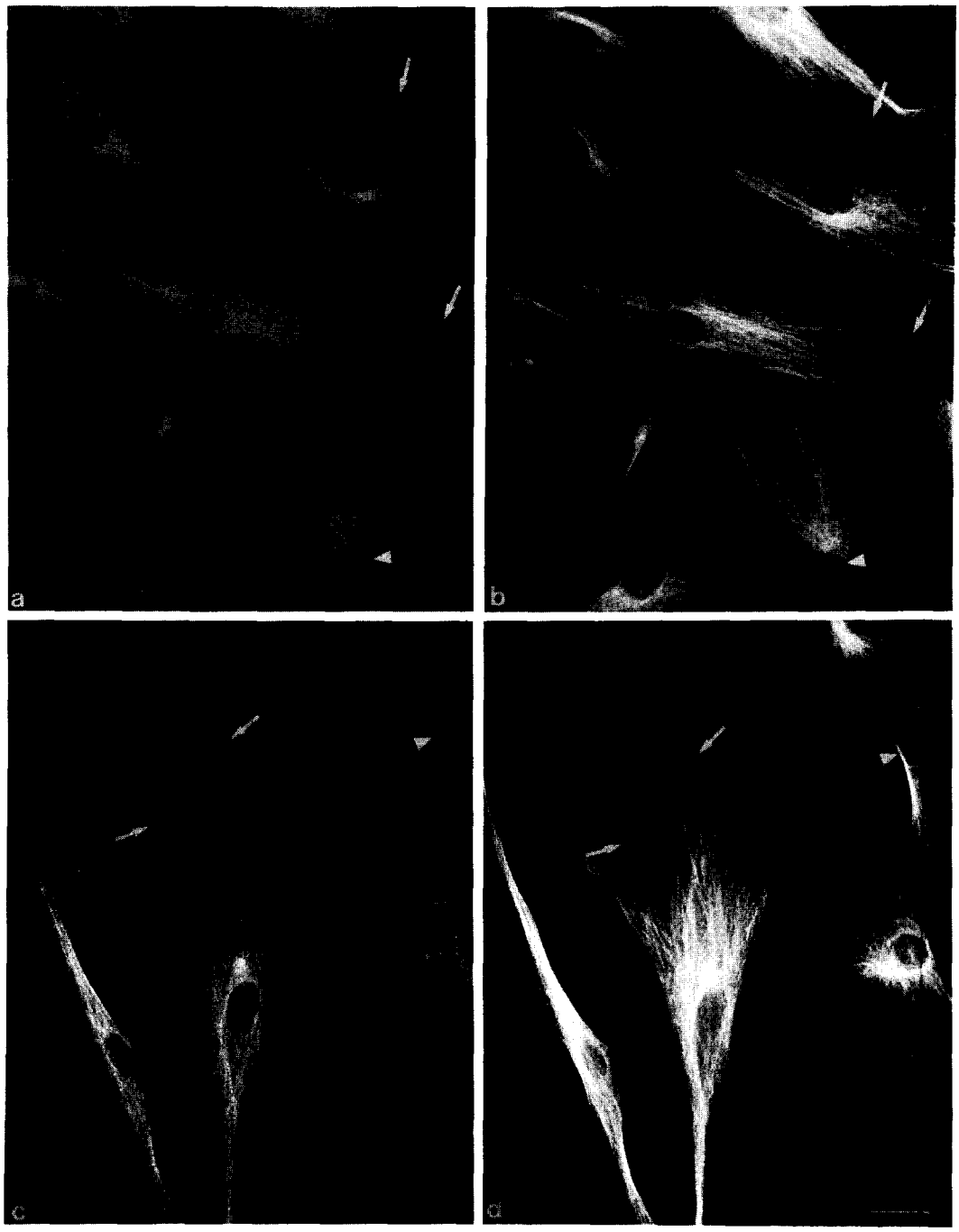

Fig. 3. Two interphase fibroblasts doublestained for GR and tubulin using two different anti-GR antibodies and conventional immunofluorescence microscopy: (a and b) GR-"mab 7" (a) and tubulin (b). (c and d) GR-"mab 1" (c) and tubulin (d). GR is well colocalized along cytoplasmic MTs (→), but is also found in the cell nuclei, however, with a slightly different staining pattern for the two anti-GR antibodies (▶). Bar corresponds to 20 μm.

very well to cytoplasmic MTs [Fig. 3(a), (b), (c) and (d)]. However, "mab 7" usually gave rise to a somewhat less sharp fibrillar pattern and also to a more diffuse background staining in the cytoplasm than "mab 1". With both "mab 1" and "mab 7", there was also often a strong GR-signal from the leading edge of the plasma membrane, which was not seen for the anti-tubulin antibody. The nuclear pattern was different between the two anti-GR antibodies; "mab 7" gave a weak, but distinct, irregular staining pattern with stained nucleoli in most cells and there was usually an intensely stained narrow zone at the nuclear periphery, possibly corresponding to the nuclear envelope. The "mab 1"-antibody signal was found in about 30% of the cell nuclei, where it showed a more granular pattern than seen with "mab 7" [cf. Fig. 3(a) and (c)]. All further CLSM-analyses were performed using solely the "mab 7" antibody.

Figure 4 shows a 1 μm thick optical, transversal section through the central part of a human gingival fibroblast, double stained for GR and tubulin. The staining pattern is similar for GR and tubulin and the same as with

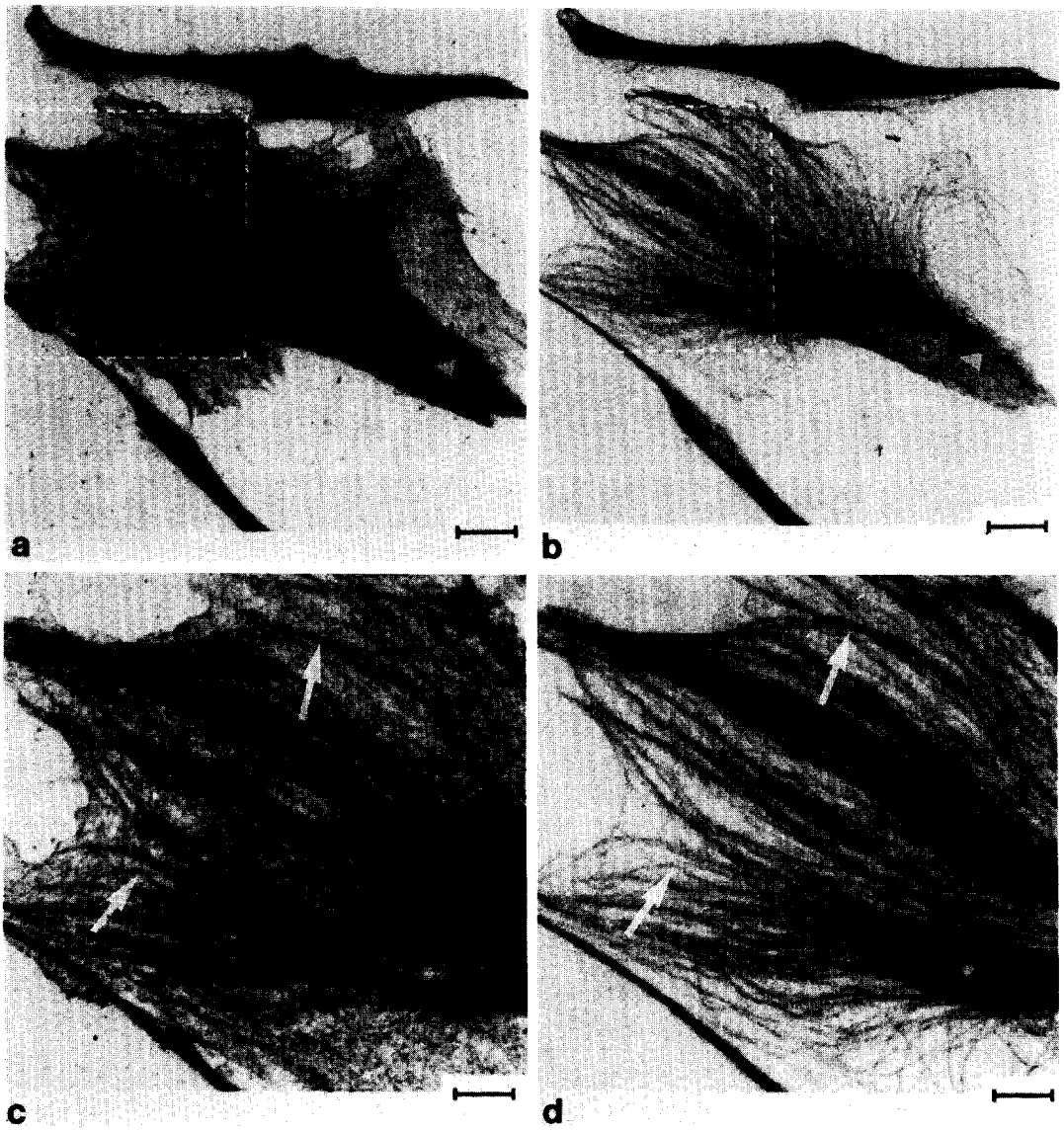

Fig. 4. Interphase fibroblasts doublestained for GR and tubulin using CLSM providing a 1 μm thick CLSM optical, transversal section through the central part of the cell: GR (a and c) and tubulin (b and d). GR and cytoplasmic MTs are closely colocalized (→). There is substantial GR staining in the nucleus and along the nuclear envelope, different from the tubulin staining (▶). c and d is a part of a and b, scanned with a smaller pixel size. Bar corresponds to 20 μm (a, b) and 10 μm (c, d), respectively.

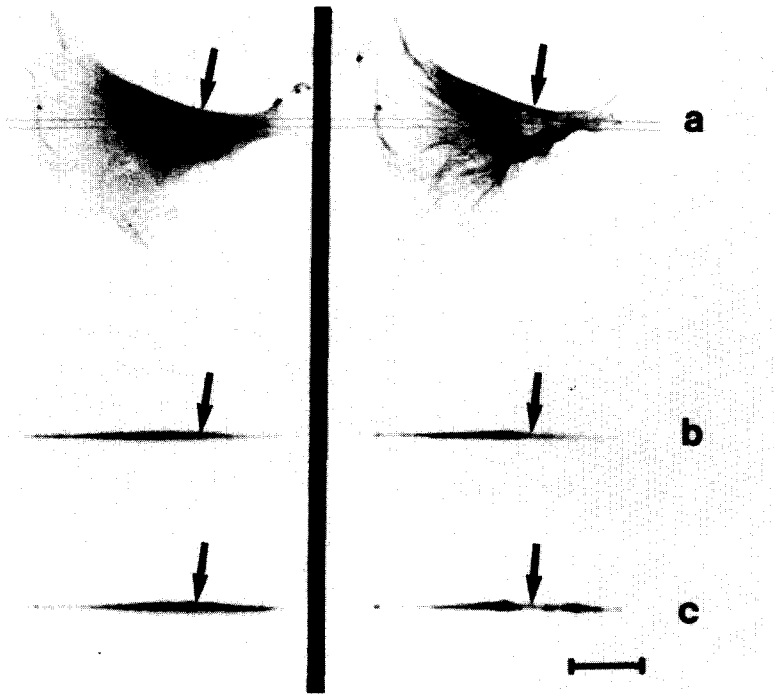

Fig. 5. Interphase fibroblast double stained for GR (left) and tubulin (right). (a) CLSM whole cell transversal projection of a stack of 10 optical sections, each about 1 μm thick. (b) Reconstructed whole cell side projection of (a). (c) Reconstructed side projection of the central 5 μm section through the cell nucleus, indicated by lines in (a). (b) and (c) are aligned with (a). The side projections reveal the flat, spread contour of the interphase fibroblast. GR is found to be colocalized with MTs in the whole cell transversal projection, but not in the two side projections. There is more GR than tubulin in the nucleus (arrows). Bar corresponds to 40 μm.

conventional fluorescence microscopy (Fig. 3). Figure 5(a) shows a whole cell transversal projection of a stack of 10 optical serial sections of a double stained fibroblast. Figure 5(b) shows an aligned reconstruction of the side projection of the same whole cell and Fig. 5(c) a reconstructed side projection of the central 5 μm section through the nucleus indicated by the dotted lines in the transversal section in Fig. 5(a). The cell was calculated to be 150 μm long, 120 μm wide and 6 μm high. The flat, spread cell shape is well shown. The fibrillar pattern of GR and tubulin is not seen in the side projections. The difference in nuclear staining for GR and tubulin is easily recognized in Fig. 5(c), i.e. there is a non-stained region corresponding to the nucleus in the tubulin-stained side projection of the 5 μm central section. The same region has a distinct GR-staining.

Figure 6 shows four optical, transversal serial sections through a fibroblast double stained for GR and tubulin. Each section is approx. 1 μm thick and the colocalization of GR and tubulin is apparent in most sections. Since the entire specimen is faded when scanning a single section, the fading will be more prominent for the last sections in a stack. In Fig. 6, the images were scanned in the sequence a–d, implying that d had faded most. As the GR-signal generally was weaker than the tubulin signal, recording GR required several more scanning-accumulations per section than tubulin, and thus the fluorescent GR–FITC-signal faded more than the tubulin–Texas Red®-signal. This may explain why the colocalization was sometimes less convincing towards the top of the cell. However, it could be concluded that the previously described fibrillar GR-distribution pattern [3] was real and not due to a projectional artifact.

Mitotic cells during basal culture conditions

Figure 7 shows a conventional immunofluorescence double staining of a mitotic fibroblast using the anti-GR antibody "mab 1" double stained with tubulin. As previously shown for "mab 7" [3], "mab 1" was colocalized with tubulin (spindle MTs) in the mitotic spindle and particularly localized to the pericentriolar regions [Fig. 7(a)]. Both anti-GR antibodies followed tubulin during all stages of the mitotic process (not shown).

Figure 8(a) shows a CLSM whole cell projection of a stack of 16 optical, transversal serial sections of two fibroblasts (one in interphase and one undergoing mitosis), double stained for GR and tubulin, as well as a side projection of the same whole cells [Fig. 8(b)] and a side projection of the central 5 μm section through the mitotic cell, indicated by the dotted lines

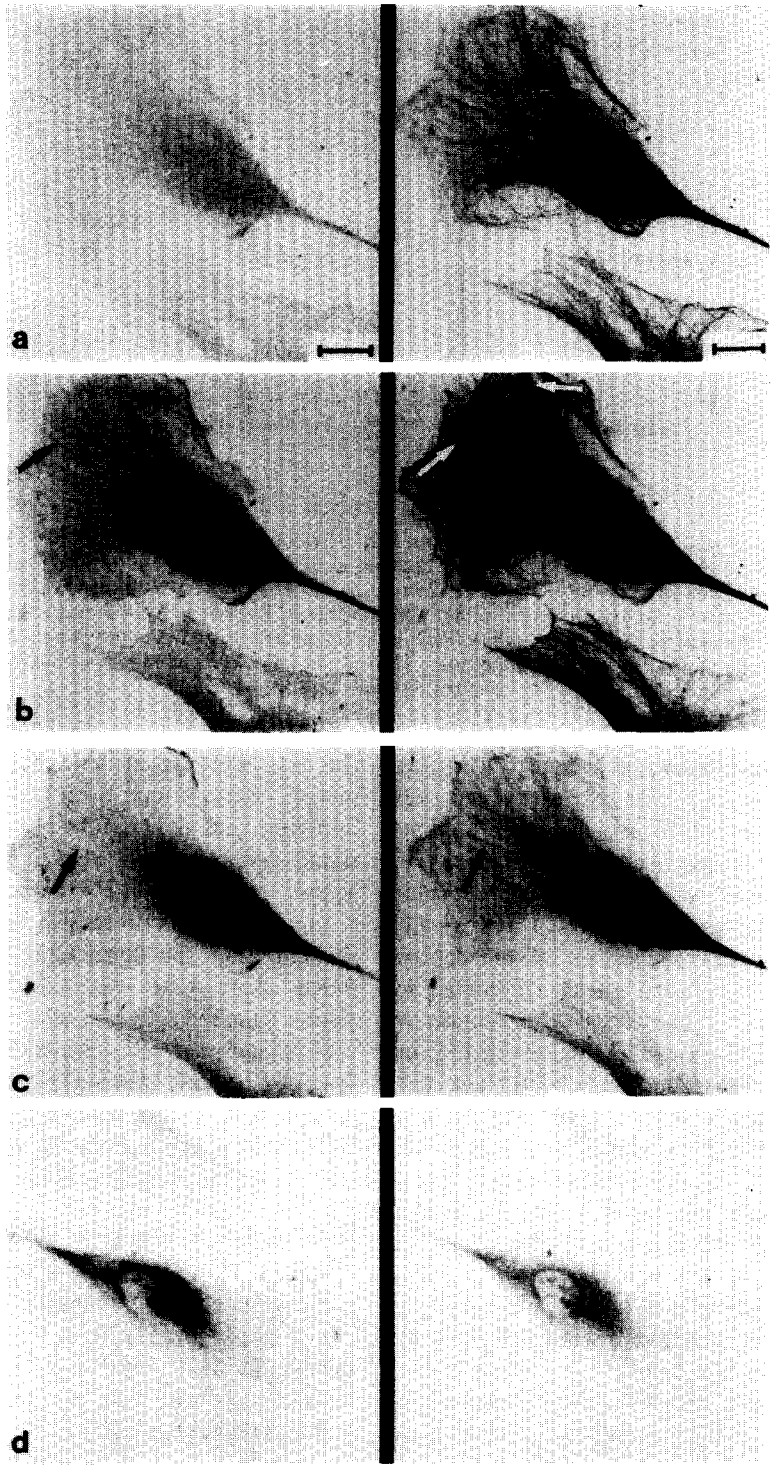

Fig. 6. Four CLSM transversal serial sections through an interphase fibroblast doublestained for GR (left) and tubulin (right). Each section is about 1 μm thick, starting at the bottom of the cell (a) and moving towards the top (d). It can be seen that the colocalization of GR and tubulin is found in several sections (→). Bar corresponds to 20 μm.

in the transversal section in Fig. 8(a) [Fig. 8(c)]. It can be seen that GR is well colocalized with tubulin in the mitotic apparatus. The GR staining seems to be more prominent than the tubulin staining in the pericentriolar regions, most easily recognized in Fig. 8(c).

Figure 9 shows four optical, transversal serial sections through a mitotic fibroblast double stained for GR and tubulin. The colocalization is apparent in all sections. In addition, GR exhibits a diffuse staining in all parts of the mitotic cell, different from tubulin.

Vinblastine treatment

Culturing the cells in the presence of 10 μM vinblastine for 1 h before fixation induced the formation of typical tubulin-containing crystalline inclusion bodies known as paracrystals [15]. These structures also contained GR. Four 1 μm thick optical, transversal serial sections through the same cell revealed that the colocalization between GR and tubulin was seen on each section (Fig. 10) and thus was not due to a projectional artifact. The paracrystals were also sometimes localized within the cell nucleus, which is in agreement with previous findings that MTs besides their cytoplasmic occurrence, are also localized within cell nuclei [16].

Subtraction analysis

To further analyze the putative structural colocalization between GR and cytoplasmic MTs, the recorded images showing the distribution of the respective structure was subtracted from each other (see Experimental). Figure 11 shows the result of a control subtraction of mouse-anti-tubulin minus rabbit-anti-tubulin [Fig. 11(c)] and vice versa [Fig. 11(d)]. As expected, both subtractions quenched most of the immunoreactivity.

In similar experiments, both GR minus tubulin [Fig. 12(c)] and tubulin minus GR [Fig. 12(d)] showed about an equally strong reduction in immunoreactivity. The GR-containing paracrystals also disappeared after GR minus tubulin subtraction (not shown). These data further supports the colocalization of GR and tubulin in these cells.

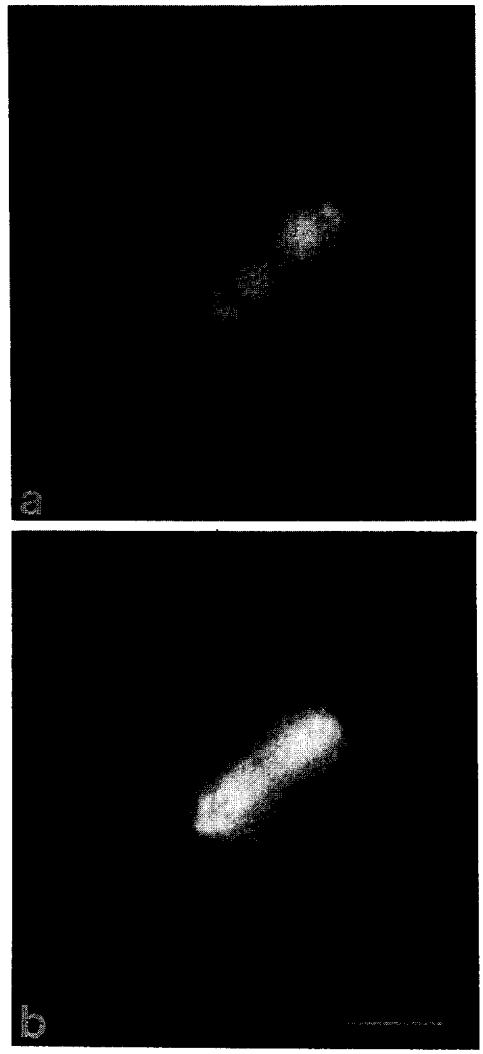

Fig. 7. Mitotic fibroblasts stained for GR and tubulin using conventional immunofluorescence microscopy. (a and b) Doublestaining for GR "mab 1" (a) and tubulin (b). The anti-GR antibody is colocalized with tubulin in the pericentriolar regions and in the mitotic apparatus in a similar manner as "mab 7" [3]. Bar corresponds to 10 μm.

DISCUSSION

The use of CLSM provides additional information compared to conventional immunofluorescence microscopy. The CSLM allows imaging of thin optical sections, approx. 1 μm in thickness, and this reduces the problem with projection artifacts in conventional fluorescence microscopy. Furthermore, CLSM allows in-focus imaging of cells of various size, e.g. interphase and mitotic cells. Besides the suppression of out-of-focus light, the confocal microscopy also yields a lateral resolution that is 1.4 times better compared to conventional microscopy [10].

The wavelength range of the argon laser used in this study is not as wide as for the mercury light. We were therefore obliged to use a wavelength of 514 nm when exciting Texas Red®, even though the optimal wavelength would be 596 nm [9]. To get a wider range of wavelengths,

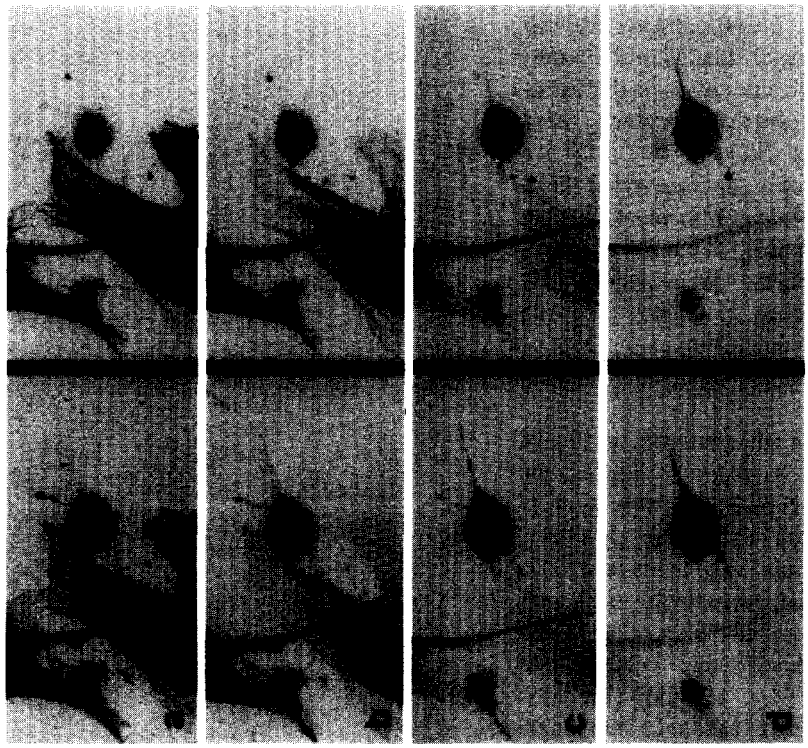

Fig. 9. Four CLSM optical, transversal serial sections through a mitotic fibroblast, doublestained for GR (left) and tubulin (right). Each section is about 1 μm thick, starting at the bottom of the cell (a) and moving towards the top (d). The colocalization of GR and tubulin in the mitotic spindle apparatus is found in each section.

Fig. 8. A mitotic and an interphase (⇒) fibroblast double stained for GR (left) and tubulin (right). (a) CLSM whole cell projection of a stack of 16 optical, transversal sections, each about 1 μm thick. (b) Reconstructed whole cell side projection of (a). (c) Reconstructed side projection of the central 5 μm section through the mitotic cell, indicated by lines in (a). (b) and (c) are aligned with (a). The side projections reveal the great difference in height between mitotic and interphase fibroblasts. GR is colocalized with tubulin in the mitotic apparatus, but is somewhat more concentrated in the pericentriolar regions than tubulin (→); this is best seen in (c). Bar corresponds to 20 μm.

a possible, but expensive, solution would be to combine the argon laser with for example a krypton laser, that provides laser light within the red region.

In this application, we obtained a good separation of FITC and Texas Red® by choosing appropriate excitation wavelengths and filter combinations that yielded an as small

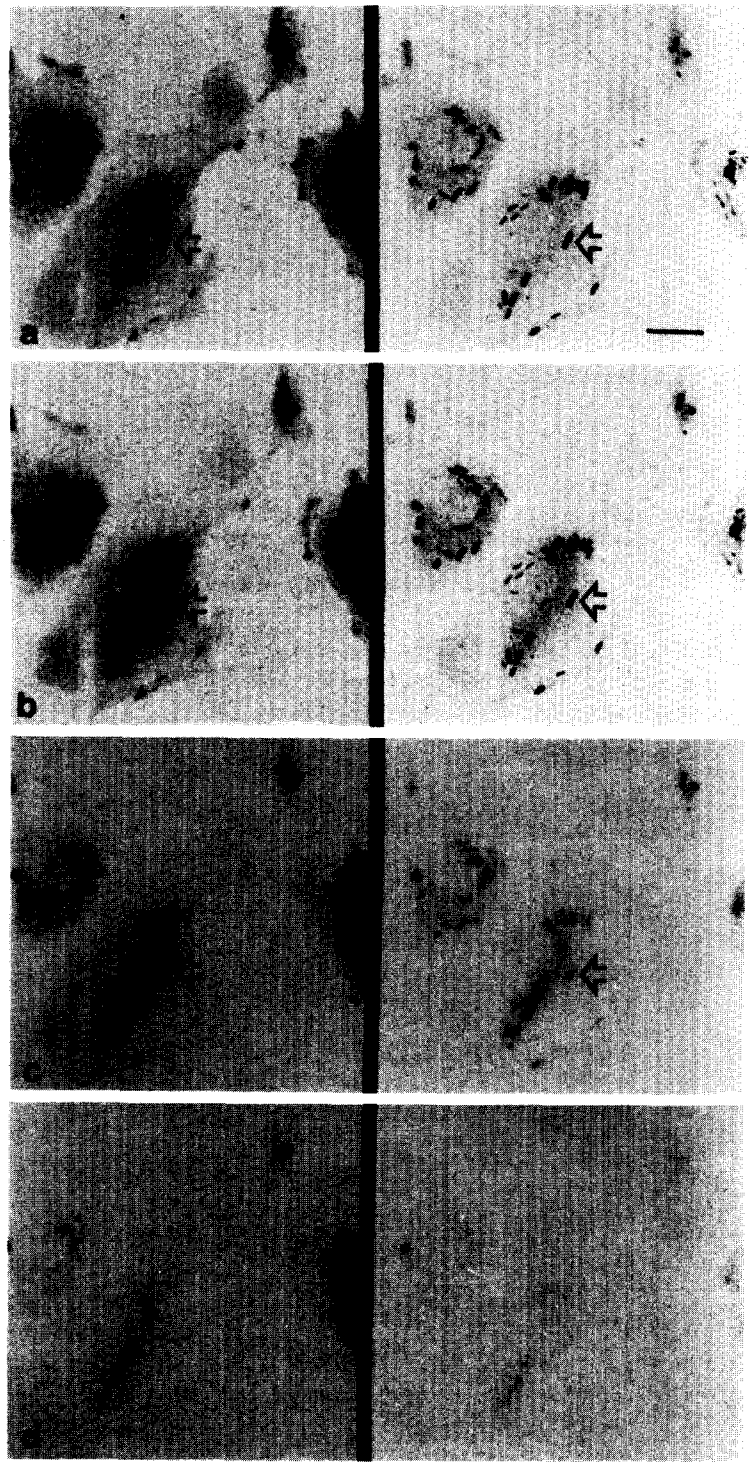

Fig. 10. Four CLSM optical, transversal serial sections through fibroblasts exposed to 10 μM vinblastine for 1 h before fixation. The cells are doublestained for GR (left) and tubulin (right). Each section is about 1 μm thick, starting at the bottom of the cell (a) and moving towards the top (d). The colocalization of GR and tubulin in vinblastine paracrystals is found in each section (⇐). Bar corresponds to 20 μm.

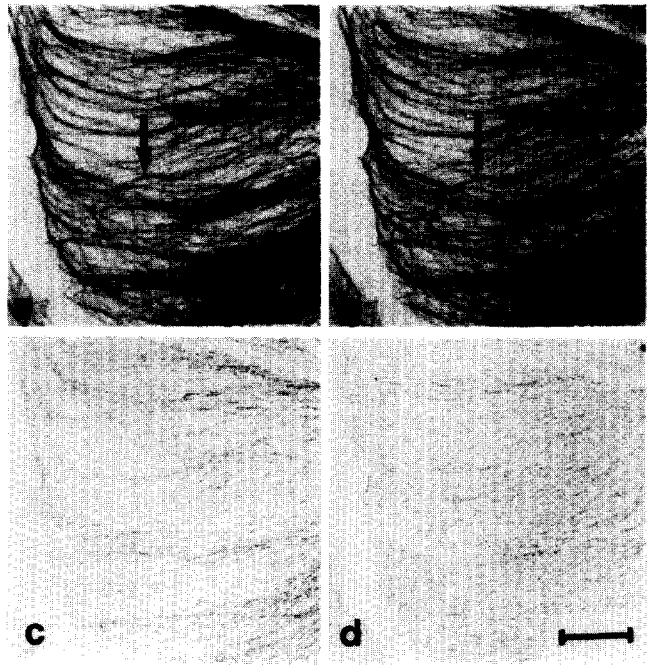

Fig. 11. Control subtraction experiment using double staining for tubulin by two different anti-tubulin antibodies produced in two different species. (a), mouse-anti-tubulin; (b), rabbit-anti-tubulin; (c), (a) – (b) and (d), (b) – (a). As expected, both subtractions quenched most of the immunoreactivity. Bar corresponds to 20 μm.

cross-talk as possible. The cross-talk (including autofluorescence) detected for monostained cells (Fig. 2) was calculated to be 5% for Texas Red® and 3% for FITC. The cross-talk is proportional to the intensity of the fluorochrome to be suppressed and not to that of the fluorochrome to be detected. This means that if, for example, the FITC-staining in Fig. 2 had been

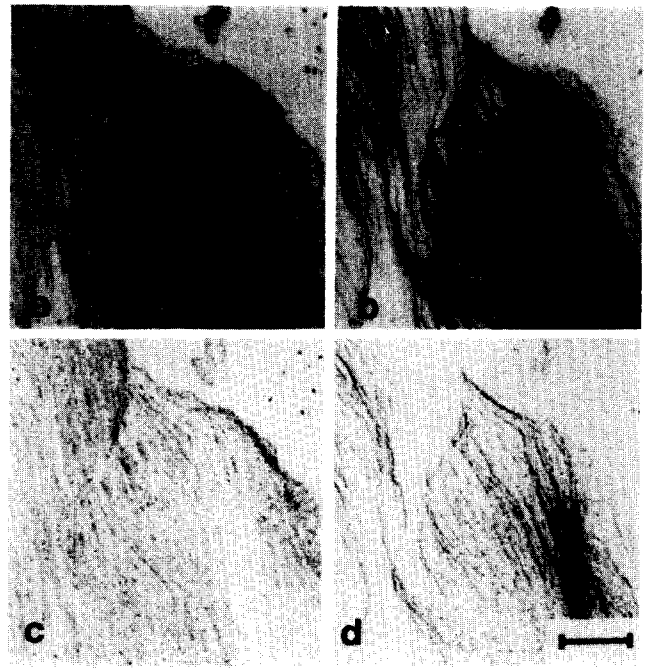

Fig. 12. Subtraction experiment, analogous to Fig. 11, using doublestaining for GR and tubulin: (a), GR; (b), tubulin; (c), (a) – (b) and (d), (b) – (a). Both subtractions showed about as strong a reduction of the immunoreactivity as in Fig. 11, supporting the notion of a close association of these structures. Bar corresponds to 20 μm.

weaker, the integration time for the FITC-recording would have to be prolonged to give a stronger signal, implying also an increase of the cross-talk from the Texas Red®-stained structures. A prerequisite for the same low cross-talk in double as in monostainings is therefore that the relative concentrations of the fluorochromes (FITC and Texas Red®) are of the same magnitude in both situations. We have no reason to assume any differences in this respect in the current study.

An observation from both conventional and CLSM immunofluorescence images to further strengthen our conclusion that we have succeeded in separating the fluorochromes in double stained specimens, is that in both interphase and mitotic cells (e.g. Figs 5 and 8) there are structures in the GR–FITC-recording that cannot be seen in the tubulin–Texas Red®-recording. Besides the well colocalized cytoplasmic MT-pattern, the GR-signal, different from tubulin, also appeared in (A) interphase cells (1) at the leading edge of the plasma membrane, (2) as a diffuse cytoplasmic background, (3) as a weak, irregular nuclear staining, (4) as stained nucleoli and (5) along the nuclear envelope, and (B) mitotic cells (1) in the pericentriolar regions (2) as a diffuse cytoplasmic background and (3) along the plasma membrane.

Another indication that what is seen in doublestained images does not represent cross-talk between fluorochromes is that monostained specimens, stained for either GR or tubulin, show the same fibrillar pattern as in the double-stained specimens. Thus, with the doublestaining technique, supplemented with CLSM, we provide further evidence for a high degree of colocalization between GR and cytoplasmic MTs.

In the method described here for detection of two fluorochromes, fluid embedded specimens may move slightly between the recordings of two cell volumes (stacks). The movements are probably due to the short working distance of the objective that allows the objective to touch the specimen via its immersion oil. This is a disadvantage if the volumes should be compared pixel by pixel. We have therefore chosen to only record a single section of the specimens in those cases where we have performed quantitative calculations, i.e. when performing subtraction analysis. Another method for detecting doublestained specimens, which gives pixel to pixel correspondence, is to simultaneously detect emitted light at two different wavelength intervals by using two detectors [17].

Since the detection of the two fluorochromes is made at the same time in the double detector system, the excitation wavelength(s) must be the same, which implies, a higher cross-talk than when two different excitation wavelengths are used. The cross-talk may be removed by subtracting a fraction of one image from the other. This requires that the magnitude of the cross-talk is known or can be calculated from a part of the images where the substances do not colocalize. This condition has not always been accomplished in our applications.

Another phenomenon that must be taken into consideration is that the focal length of the objective may differ for different wavelengths due to chromatic aberration. This focus shift will cause disalignment of the serial sections registered with different wavelengths for different fluorochromes. We have measured the focus shift to 0.4–0.5 μm for our $\times 63$ plan-apochromat objective when changing the wavelength from 476 to 514 nm during the scanning of a mirror with reflective light. However, the magnitude of the focus shift does not need to be the same when recording a fluorescent specimen, where not only the exciting wavelengths differ, but also the fluorescent wavelengths. The effects of the disalignment between two sections are most prominent when studying thin structures with a thickness less than the thickness of the optical section. We have not found these effects to be a problem in our study.

The results presented here strengthen the conclusion raised in our previous paper of a structural interaction between GR and cytoplasmic MTs in human gingival fibroblasts. The two different monoclonal anti-GR antibodies gave rise to a very similar staining pattern correlating very well with the localization of cytoplasmic MTs. GR and tubulin are colocalized in 1 μm thick sections in interphase cells, mitotic cells and in vinblastine induced paracrystals. Subtraction of the GR-signal from that of tubulin and vice versa strongly reduced the visible immunoreactivity of the respective structure. Thus, GR seems to follow the spontaneous redistribution of MTs during the cell cycle and also during the artificial redistribution of MTs into vinblastine induced paracrystals.

The physiological significance of an interaction between GR and MTs is at the present unclear. One possibility is that, during interphase, GR might use MTs as transportation

tracks for its movement into the nucleus after binding of a glucocorticoid hormone [18]. Presently, we have no explanation for the localization of GR in the mitotic spindle and especially in the pericentriolar regions. There are previous immunofluorescence studies claiming that glucocorticoid hormones are localized in the pericentriolar regions [19].

Glucocorticoids are known to influence cell growth. The effect varies in different cell types and the data is somewhat contradictory. In fibroblasts, both stimulatory and inhibitory effects on growth have been reported [20]. It is an attractive notion that glucocorticoids might regulate cell growth by having their receptor localized in close proximity to the mitotic apparatus.

Acknowledgements—The valuable help from the constructive and stimulating discussions with Dr Kjell Carlsson and Professor Nils Åslund, Physics IV, The Royal Institute of Technology is greatly appreciated. This work was supported by Grants from the Swedish Medical Research Council (No. 13x-2819) and from the Swedish Cancer Society (No. 1940). Ann-Charlotte Wikström is a recipient of a fellowship from the Swedish Medical Research Council.

REFERENCES

1. Wrange Ö., Okret S., Radojcic M., Carlstedt-Duke J. and Gustafsson J.-Å.: Characterization of the purified activated glucocorticoid receptor from rat liver cytosol. *J. Biol. Chem.* **259** (1984) 4534–4541.
2. King W. J. and Greene G. L.: Monoclonal antibodies localize estrogen receptor in the nuclei of target cells. *Nature* **307** (1984) 745–747.
3. Akner G., Sundqvist K.-G., Denis M., Wikström A.-C. and Gustafsson J.-Å.: Immunocytochemical localization of glucocorticoid receptor in human gingival fibroblasts and evidence for a colocalization of glucocorticoid receptor with cytoplasmic microtubules. *Eur. J. Cell Biol.* **53** (1990) 390–401.
4. Fuxe K., Wikström A.-C., Okret S., Agnati L. F., Härfstrand A., Yu Z.-Y., Granholm L., Zoli M., Vale W. and Gustafsson J.-Å.: Mapping of glucocorticoid receptor immunoreactive neurons in the rat tel- and diencephalon using a monoclonal antibody against rat liver glucocorticoid receptor. *Endocrinology* **117** (1985) 1803–1812.
5. Wikström A.-C., Bakke O., Okret S., Brönnegård M. and Gustafsson J.-Å.: Intracellular localization of the glucocorticoid receptor: evidence for cytoplasmic and nuclear localization. *Endocrinology* **120** (1987) 1232–1242.
6. Picard D. and Yamamoto K. R.: Two signals mediate hormone-dependent nuclear localization of the glucocorticoid receptor. *EMBO Jl* **11** (1987) 3333–3340.
7. Okret S., Wikström A.-C., Wrange Ö., Andersson B. and Gustafsson J.-Å.: Monoclonal antibodies against the rat liver glucocorticoid receptor. *Proc. Natn. Acad. Sci. U.S.A.* **81** (1984) 1609–1613.
8. Brönnegård M., Poellinger L., Okret S., Wikström A.-C., Bakke O. and Gustafsson J.-Å.: Characterization and sequence-specific binding to mouse mammary tumor virus DNA of purified activated human glucocorticoid receptor. *Biochemistry* **26** (1987) 1697–1704.
9. Titus J. A., Haugland R., Sharrow S. O. and Segal D. M.: Texas Red®, a hydrophilic, red-emitting fluorophore for use with fluorescein in dual parameter flow microfluorometric and fluorescence microscopic studies. *J. Immun. Meth.* **50** (1982) 193–204.
10. Wilson T. and Sheppard C.: *Theory and Practice of Scanning Optical Microscopy*. London Academic Press (1984).
11. Åslund N., Carlsson K., Liljeborg A. and Majlöf L.: PHOIBOS, a microscope scanner designed for microfluorimetric applications, using laser induced fluorescence. In *Proceedings, Third Scandinavian Conference of Image Analysis*. Studentlitteratur, Lund, Sweden. (1983) pp. 338–343.
12. Carlsson K. and Åslund N.: Confocal imaging for 3-D digital microscopy. *Appl. Opt.* **26** (1987) 3232–3238.
13. Mossberg K. and Ericsson M.: Detection of doubly stained fluorescent specimens using confocal microscopy. *J. Microscopy* **158** (1990) 215–224.
14. Forsgren P.-O.: Visualization and coding in three dimensional image processing. *J. Microscopy* **159** (1990) 195–202.
15. Fujiwara K. and Tilney L. G.: Substructural analysis of the microtubule and its polymorphic forms. *Ann. N.Y. Acad. Sci.* **253** (1975) 27–50.
16. Dustin P.: *Microtubules*. Springer-Verlag, Berlin (1984) p. 111.
17. Carlsson K.: 3D representation of microscopic specimens using confocal laser microscopy and digital image processing. Proceedings/SPIE Vol. 1245 Biomedical image processing (1990).
18. Pratt W. B., Redmond T., Sanchez E. R., Bresnick E. H., Meshinchi S. and Welsh M. J.: Speculations on the role of the 90kDa heat shock protein in glucocorticoid transport and function. In *The Steroid/Thyroid Hormone Receptor Family and Gene Regulation*. Proc. 2nd Int. CBT Symp. Stockholm, Sweden, Nov. 1988 (Edited by J. Carlstedt, H. Eriksson and J.-Å. Gustafsson). Birkhäuser Verlag, Berlin (1989), pp. 109–126.
19. Nenci I. and Marchetti E.: Concerning the localization of steroids in centrioles and basal bodies by immunofluorescence. *J. Cell Biol.* **76** (1978) 255–260.
20. Durant S., Duval D. and Homo-Delarche F.: Factors involved in the control of fibroblast proliferation by glucocorticoids: a review. *Endocrine Rev.* **7** (1986) 254–269.